

Numerical analysis of magnetic field effects on the heat transfer enhancement in ferrofluids for a parabolic trough solar collector

Ali Khosravi ^a, Mohammad Malekan ^{b,*}, Mamdouh E.H. Assad ^c

^a Department of Mechanical Engineering, School of Engineering, Aalto University, Finland

^b Division of Bioengineering, Heart Institute (InCor), Faculty of Medicine, University of São Paulo, Brazil

^c Department of Sustainable and Renewable Energy Engineering, University of Sharjah, United Arab Emirates

ARTICLE INFO

Article history:

Received 26 May 2018

Received in revised form

25 September 2018

Accepted 4 November 2018

Available online 7 November 2018

Keywords:

Parabolic trough collector

Solar thermal power plant

Fe₃O₄ nanoparticles

Heat transfer coefficient

CFD simulation

ABSTRACT

A parabolic trough is defined as a type of solar thermal collector that is straight in one dimension and curved as a parabola in the other two, lined with a polished metal mirror. Enhancing the thermal efficiency of this collectors is one of the major challenges of developing and growing of parabolic trough solar thermal power plants. Ferrofluids were proposed as a novel working fluid for industrial applications, due to their thermal performances. In this study, the convective heat transfer of Fe₃O₄-Therminol 66 ferrofluid under magnetic field (0–500 G) is evaluated using computational fluid dynamics. The ferrofluid with different volume fraction (1–4%) and the Therminol 66 (as the base fluid) are considered as the working fluids for a parabolic trough solar collector. Numerical analysis first validated using theoretical results, and then a detailed study is conducted in order to analyze the effect of the magnetic field on different parameters. The result demonstrated that using magnetic field can increase the local heat transfer coefficient of the collector tube, thermal efficiency as well as output temperature of the collector. In addition, increasing the volume fraction of nanoparticle in the base fluid and intensity of magnetic field increased the collector performance.

© 2018 Elsevier Ltd. All rights reserved.

1. Introduction

Renewable energy, for instance solar and wind energy, is one of the most promising solutions to produce clean energy for the future since the conventional energy sources (such as oil, coal and natural gas) will be finished in a few decades [1,2]. World energy consumption is increasing continually and this is worrisome for all researchers and scientists [3]. Solar energy, as an abundant energy source, can either be converted into heat or electricity. It is a useful source of energy for various applications: solar dryers, local hot water production, and electricity production in concentrating solar power plants [4]. Global solar energy production was predicted to reach a rate of 8.9% annually between 2012 and 2040, making it the fastest developing type of energy generation in the forthcoming decades [5].

Different types of solar collectors have been used to absorb solar energy, such as: evacuated tubes, flat plate black-surface absorbers,

and parabolic trough solar collector (PTSC) [6,7]. PTSC is a solar concentrating system which utilizes a parabolic reflector to concentrate solar radiation onto a solar absorbing pipe made of metal materials [8]. It is the most suitable technology with high thermal efficiency, for operation in medium to high-temperature levels (over 150 °C) [6]. A working fluid flows through the absorber pipe and the heat from the pipe is transferred to this fluid. Typically, the working fluid is selected from the thermal oils, such as Therminol, Dowtherm, Syltherm and Sandotherm, in which they can operate up to 400 °C [9]. The vast majority of the PTSC working fluids are Therminol VP1 and Syltherm 800 thermal oil, because of their reliability and accessibility [10].

The heat transfer performance is mainly dependent on the thermal conductivity as well as specific heat of the working fluids. Therefore, by increasing the fluid thermal conductivity/specific heat, the heat transfer performance would be improved. Nanoparticles provide an effective way of improving heat transfer characteristics of working fluids [11]. Choi [12] was found for the first time that nanoparticles increase the thermal conductivity of the coolant, therefore improving the heat transfer performance. Nanofluids are comprised of a concentration of nanoscale-sized

* Corresponding author.

E-mail addresses: mmalekan1986@gmail.com, malekan@dees.ufmg.br (M. Malekan).

particles, including pure metals; oxides; carbides; and carbon nanotubes, immersed in a base fluid [13].

There are a bunch of numerical investigations dealing with effect analysis of using nanofluids on the thermal efficiency of the PTSCs. Otanicar et al. [14] have experimentally and numerically investigated the effect of different nanofluids on the performance of a direct absorption collector. Kasaeian et al. [15] and Sokhansefat et al. [16] have numerically studied the fully developed turbulent mixed convection heat transfer (CHT) of the Al_2O_3 /synthetic oil nanofluid in a PTSC, with a uniform and non-uniform heat fluxes, respectively. Their results showed that the Nusselt number as well as the convection heat transfer coefficients (HTC) are dependent on the nanofluid volume fraction. Xu et al. [17] have presented an investigation of the operating characteristics of a novel nanofluid-based direct absorption solar collector under solar-concentrating medium-temperature operating conditions. They have used CuO-oil as the working fluid and found out that the direct absorption collector had a better performance than indirect one. Bellos et al. [18] have studied the thermal efficiency enhancement of the commercial parabolic collector using three different working fluids: thermal oil, thermal oil with nanoparticles and pressurized water. Their results have indicated that the use of nanofluids increases the collector efficiency by 4.25%. Amina et al. [19] have presented a 3D numerical model to investigate the heat transfer in a PTSC receiver with longitudinal fins using different kinds of nanoparticles (Al_2O_3 , CuO, Sic, and a nonmetal particle). Their results have shown that the Nusselt number increased from 1.3 to 1.8 times, and also the metallic nanoparticles increase heat transfer significantly than other nanoparticles. Kaloudis et al. [7] have studied the convective heat transfer of Al_2O_3 /synthetic 800 nanofluid in a PTSC using two-phase model computational fluid dynamics (CFD) simulation. Their results have reported a maximum relative error for outlet temperature about 0.3% and a growth up to 10% on the collector efficiency with the 4% volume fraction of nanoparticles. Ghasemi et al. [20,21] have presented the effect of Al_2O_3 -water and Al_2O_3 -Therminol 66 nanofluids on the efficiency of PTSC using CFD simulations. Their results have indicated that the nanofluid enhanced the heat transfer performance and bigger nanoparticle volume fraction leads to increase in Nusselt number. Kasaeian et al. [22] have reviewed the nanofluid applications in solar energy systems, and also Gorji and Ranjbar [23] have presented an extensive review of the literature regarding the use of nanofluids in direct absorption PTSCs.

Ferrofluid which is composed of magnetic nanoparticles such as nickel, iron, cobalt and their oxides, is able to improve the heat transfer coefficient in the presence of magnetic field. These magnetic nanofluids are proposed as working fluid for different types of heat exchangers, heat transfer enhancement for cooling of high powers and heat pipes [24]. The use of ferrofluid under the right magnetic field increases the thermal conductivity of the fluid which results in better heat transfer performance of the parabolic trough solar collector. The solute particle magnetic property in fact is behind the enhancement of the thermal conductivity which can be controlled by applying external magnetic field. Moreover, the ferrofluid viscosity can be controlled by the magnetic field applied. The enhanced thermal conductivity of ferrofluid results in improving the heat conduction during chain-like particle assembly formation under the external magnetic field [25,26]. There are different numerical investigations of the ferrofluids HTC performance with/without presence of the magnetic field: Jafari et al. [27] have simulated the heat transfer of a ferrofluid under a magnetic field based on kerosene into a cylinder; Huminic et al. [28] numerically examined the heat transfer of nanofluid in a helical double pipe heat exchanger in laminar flow; Aminossadati et al. [29] studied laminar forced CHT of Al_2O_3 /water nanofluid in a

horizontal micro-channel; Malekzadeh et al. [30] presented a numerical analysis of the effect of magnetic field on HT in a laminar flow through a tube; Aminfar et al. [31–34] numerically investigated in several works the effect of non-uniform transverse/axial magnetic fields on hydro-thermal as well as hydro-dynamic behaviors of ferrofluids; magnetic field effects on natural CHT of copper/water and copper oxide/water nanofluids were numerically investigated by Sheikholeslami et al. [35] and Mahmoudi et al. [36], respectively; magnetic field effects on the convection onset for the nanofluid were examined by Yadav et al. [37–39]; and Shakiba et al. [40] numerically studied the hydro-thermal characteristics of water/ Fe_3O_4 ferrofluid in a double pipe heat exchanger, which was exposed to a variable magnetic field intensities. These studies have reported one common outcome which is presence of magnetic field leads to increasing the heat transfer performance, and hence the Nusselt number. More recently, Malekan et al. [41] and Khosravi et al. [42] have investigated the effect of magnetic field on the HTC using computational fluid dynamics and adaptive neuro-fuzzy inference system.

Parabolic trough collector is introduced as the most proven technology for indirect steam generation in solar thermal power plants. Although this technology for electricity generation is not yet competitive with fossil fuel power plants in some countries, it is one of the economically feasible renewable energy technologies in the future. Hence, obtaining the better performance of this system is defined as a challenge for researchers. During the last decades, an extensive research work has been done on the fluids dynamics in the presence of magnetic field. The effect of magnetic field on fluids is worth investigating due to its innumerable applications in different fields. Based on the literature review, many investigations were developed numerically to predict the HTC of nanofluids in parabolic trough solar collector, and also many experimental and numerical investigations to study the effect of ferrofluids on the heat transfer performance in pipes and heat exchangers. But, there are no numerical investigations regarding the effect of ferrofluids on the convective HTC performance in the PTSCs, in the presence of magnetic fields. The aim of the current study is to numerically examine the thermal performance of solar parabolic trough collector with ferrofluid under constant magnetic field. The ferrofluid is considered with different volume fraction. The numerical simulation is executed using the capabilities of CFD approach embedded in ANSYS Fluent 18.2.

2. Problem definition

Schematic of the solar parabolic trough collector system is shown in Fig. 1. The solar radiation is concentrated into the receiver tube by a parabolic concentrator, and it is transmitted to the

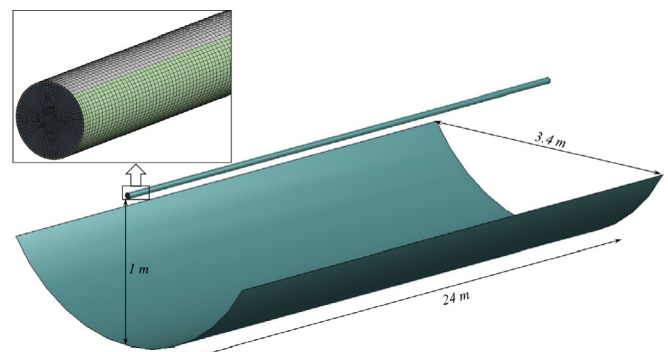


Fig. 1. Geometry of the examined model of parabolic trough collector.

working fluid by convection heat transfer. Ferrofluid helps to have a better heat transfer characteristics for the parabolic trough collector.

The local concentration ratio in the absorber tube is shown in Fig. 2, which means only lower half of the tube is receiving the concentrated solar radiation reflected by the collector. This radiation will be applied over tube outer wall as heat flux, within our numerical simulation.

The magnetic field is generated by an electric current going through a wire parallel to the absorber tube longitudinal axis, below the tube outer wall. The current-carrying wire would cause a non-uniform transverse magnetic field perpendicular to the ferrofluid flow direction.

2.1. Ferrofluid physical properties

Ferrofluid (ff) properties are dependent on the volumetric fraction of the nanoparticles (vol %, i.e. ϕ). The ferrofluid properties can be obtained from using a set of equations, which depend on the physical properties of nanoparticles (p) and base fluid (f). Ferrofluid density, specific heat capacity, thermal conductivity, and dynamic viscosity are presented by [16,18,43,44]:

$$\rho_{ff} = (1 - \phi)\rho_f + \phi\rho_p \quad (1)$$

$$C_{p,ff} = (1 - \phi)C_{p,f} + \phi C_{p,p} \quad (2)$$

$$\mu_{ff} = (1 + 2.5\phi)\mu_f \quad (3)$$

$$k_{ff} = \left(\frac{k_p + (n - 1)k_f - (n - 1)\phi(k_f - k_p)}{k_p + (n - 1)k_f + \phi(k_f - k_p)} \right) k_f \quad (4)$$

where ρ is the density, C_p is the specific heat, μ is the dynamic viscosity and k is the thermal conductivity. Subscript ff in Eqs. (1)–(4) stands for the ferrofluid. Equation (4) was presented for the first time by Hamilton & Crossor [45], and n is the shape factor which is 3 for spherical particles.

Ferrofluid in this study is a mixture of Theminol 66 and Fe_3O_4 nanoparticles, with the different volumetric fractions. The usual range values for this parameter is 0.1–4% [46]. The nanoparticles are spherical with a diameter of about 10 nm. Table 1 presents the properties of the nanoparticles, base fluid and of the ferrofluid.

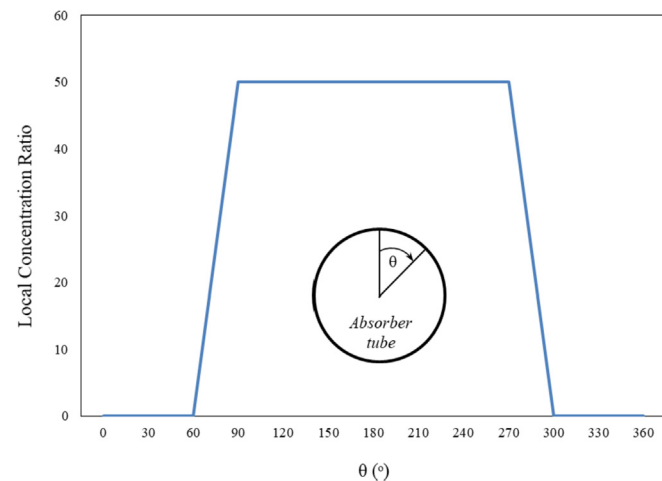


Fig. 2. Local concentration ratio distribution in the absorber tube.

Table 1
Thermo-physical properties of materials.

Material	$\rho(\text{kg}/\text{m}^3)$	$C_p(\text{J}/\text{kg}\cdot\text{K})$	$k(\text{W}/\text{m}\cdot\text{K})$	$\mu(\text{kg}/\text{m}\cdot\text{s})$
Theminol 66 (base fluid)	899.5	2122	0.107	0.00106
Fe_3O_4 (particle)	5200	670	6	–
Ferrofluid with 1 vol %	942.5	2107.48	0.110073	0.0010865
Ferrofluid with 2 vol %	985.5	2092.96	0.113206	0.001113
Ferrofluid with 4 vol %	1071.5	2063.92	0.119657	0.001166

2.2. Heat transfer analysis

The heat transfer from the absorber to working fluid is the core of the analysis and depends on the heat convection coefficient. Larger values of this parameter lead to lower absorber temperature, and hence lower thermal heat losses. Parabolic trough collectors utilize the direct beam solar irradiation (G_b). Thus, the available solar irradiation in the collector module (Q_s) is calculated as the product of the direct beam solar irradiation and collector aperture (A_a):

$$Q_s = A_a \cdot G_b \quad (5)$$

The useful heat (Q_u) absorbed by the working fluid is calculated by the energy balance in the fluid volume according to:

$$Q_u = \dot{m} \cdot c_p \cdot (T_{out} - T_{in}) \quad (6)$$

The thermal efficiency of the solar collector is calculated as the ratio of the useful thermal energy to the available solar irradiation, using following equation:

$$\eta_{th} = \frac{Q_u}{Q_s} \quad (7)$$

In theoretical basis, the convection heat transfer coefficient (h) is calculated by the Nusselt number which depends on the flow conditions and the problem geometry [47]. Nusselt number is defined as:

$$Nu = \frac{hD_i}{k} \quad (8)$$

By having the pressure drop along the absorber tube, the friction factor (f) can be calculated according to the following relation [48]:

$$f = \frac{2\Delta P}{\rho_{ff} u^2} \left(\frac{D_i}{L} \right) \quad (9)$$

where ΔP is the pressure drop, L is the tube length, and u is the fluid velocity. The theoretical value for the friction factor can be calculated using the Petukhov relation, as [49]:

$$f = (0.79 \cdot \ln Re - 1.64)^{-2} \quad (10)$$

According to Webb [50], an effective way to evaluate the thermo-hydraulic behavior of ferrofluid flow in the heat exchanger or solar receiver is to use the performance evaluation criteria (PEC) which is defined as follows:

$$PEC = \frac{Nu/Nu_0}{(f/f_0)^{1/3}} \quad (11)$$

in which Nu_0 and f_0 are the Nusselt number and friction factor of the receiver tube having base fluid as the working fluid, respectively, where f and Nu are the friction factor and the Nusselt number of the receiver tube with ferrofluids, respectively.

2.3. Magnetic field and governing equations

Suppose that the particles are dispersed in the base fluid, and therefore because of their small size, they act like a fluid. In addition, by assuming that the slipping velocity between nanoparticles and base phase is negligible, ferrofluid can be considered as a single-phase fluid with physical properties based on two-component concentration, i.e. base fluid and nanoparticles. Therefore, continuity, momentum, and energy equations of a pure fluid are applicable to a ferrofluid, except that the effective properties of ferrofluid must replace the base fluid properties. Components of a magnetic field generated by a wire that carries electric current (I) can be calculated as [51]:

$$H_x(x, y) = \frac{I \cdot (x - a)}{2\pi [(y - a)^2 + (x - b)^2]} \quad (12)$$

$$H_y(x, y) = \frac{I \cdot (y - b)}{2\pi [(y - a)^2 + (x - b)^2]} \quad (13)$$

where, the magnetic intensity can be calculated as follows:

$$H(x, y, z) = H(x, y) = \frac{I}{2\pi \sqrt{(y - a)^2 + (x - b)^2}} \quad (14)$$

Conservation equations can be stated as follows by considering a steady and incompressible flow; constant thermo-physical properties, and negligible viscosity:

$$\text{Continuity equation: } \nabla \cdot (\rho_{ff} \vec{v}_{ff}) = 0 \quad (15)$$

$$\begin{aligned} \text{Momentum equation: } \nabla \cdot (\rho_{ff} \vec{v}_{ff}) \\ = -\nabla p + \nabla (\mu_{ff} \nabla \vec{v}_{ff}) + \mu_0 (\vec{M} \cdot \nabla) \vec{H} \end{aligned} \quad (16)$$

$$\text{Energy equation: } \rho_{ff} C_{p,ff} \left(\frac{\partial T}{\partial t} + \vec{v}_{ff} \cdot \nabla T \right) = k_{ff} \nabla^2 T \quad (17)$$

in which μ_0 is magnetic permeability constant in vacuum. The term $\mu_0 (\vec{M} \cdot \nabla) \vec{H}$ is the Kelvin force which will be zero if there is no gradient of the magnetic field.

The magnetic field generated by a steady current, I, can be obtained by the Biot–Savart law:

$$B = \frac{\mu_0 I}{2\pi r} \quad (18)$$

in which, r is the distance between the location of wire and the location where the magnetic field is calculated. For the current study, the parameter r is the distance between the wire and the tube longitudinal axis.

2.4. Boundary conditions

The following boundary conditions are applied to the receiver tube numerical model:

■ Inlet

The fluid flow has a uniform velocity and uniform temperature at the receiver inlet:

$$u = u_0, T_f = T_0 = 230^\circ \text{C} \quad (19)$$

■ Wall

A uniform heat flux is applied at the outer surface of the receiver. Top and bottom half periphery of the receiver are subjected to:

$$\dot{q}_{up} = I_g \quad (20)$$

$$\dot{q}_{down} = I_b C_R \quad (21)$$

where, I_g is global radiation and is considered equal to 700 W/m², I_b is beam radiation and considered equal to 650 W/m², and C_R is the collector concentration ratio and is assumed equal to 30.

■ Outlet

Zero pressure gradient condition is employed across the outlet boundary.

3. Results and discussion

Governing equations are solved using the commercial software ANSYS® Fluent® 18.2. The effects of magnetic field on hydro-thermal characteristics of the fluid are investigated by applying a single phase model. A 3D steady state turbulent k–ε RNG model along with standard wall functions is used to simulate the heat transfer in the receiver tube. The RNG derived k–ε model gives very good predictions for a pipe and when non-equilibrium wall functions are implemented [52]. Therefore k–ε RNG turbulent model along with the SIMPLEC solution algorithm [53] are adapted for the parabolic trough receiver system. The second order upwind differencing scheme is used for momentum and energy equations. The convergence limits are set to be equal to 10^{−3} for momentum and mass and 10^{−6} for energy equations. The ferrofluid properties and magnetic field effects are incorporated within the simulation using a user-defined function code written in C language.

A mesh sensitivity analysis is made for the receiver tube and thermal efficiency of solar collector is calculated for different meshes. Table 2 gives the results of the mesh sensitivity analysis, in which it is performed for the smooth absorber and for inlet temperature equal to 230 °C. Finally, a mesh with around 4.5 million cells is selected as an appropriate discretization.

3.1. Validity study

Fig. 3 shows friction factor variation obtained from the current model. Results from current simulation were calculated using Eq. (9), by having the pressure drop and velocity for each case, and theoretical result was obtained using Eq. (10). As it can be seen from this figure, the present CFD results agree well with the theoretical outputs, with a maximum error of 2%.

Table 2
Mesh independency analysis.

Cells	671,467	1,239,200	2,373,828	3,404,164	4,522,038
η_{th}	0.7272	0.7285	0.7314	0.7321	0.7324

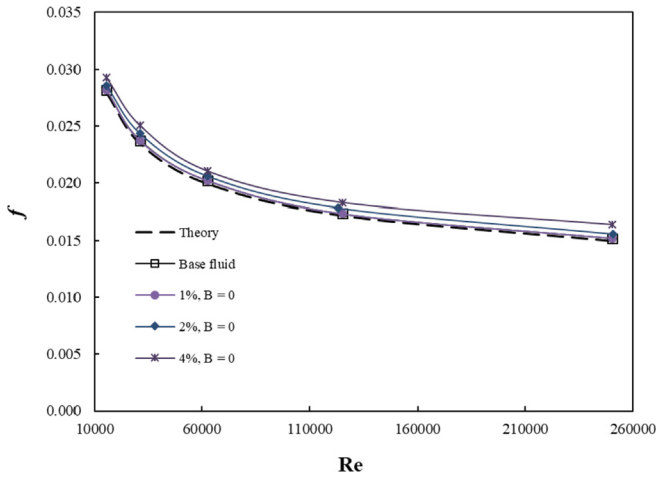


Fig. 3. Friction factor variation to validate the present model with Petukhov correlations [49].

3.2. CFD results

As it was stated before, ferrofluid with different volume fraction (1%, 2%, and 4%) is used as the working fluid. In addition, a current-

carrying wire is located close to the collector tube, aiming to provide magnetic field for the nanoparticles. Fig. 4 presents outlet temperature and velocity for the base fluid (Therminol 66), under inlet temperature 503 K and Re of 15000 and 31000, respectively.

Figs. 5 and 6 present outlet temperature, for a flow with the inlet temperature of 503 K, magnetic field intensities of $B = 0$ G, and 500 G, and for $Re_{ff} = 15000$. Although, surface temperature for the tube without magnetic field reaches a bigger value than in the presence of magnetic field, magnetic field helps to have the majority of fluid flows with the higher temperature.

Figs. 7 and 8 present the velocity streamline at the collector tube outlet, along with a magnetic field of $B = 500$ G and without magnetic field, for ferrofluid Reynolds of $Re_{ff} = 15000$, and for different volume fractions. Similar to the outlet temperature distributions, applying the magnetic field results in diffusion of the outlet boundary layer to the central parts of the tube. As it can be seen from Fig. 7, the generated force in the transverse plane grows by increasing the magnetic field intensity, which results in secondary flows, and then two vortices. While in the case of ferrofluid without magnetic field, the maximum velocity at the output is concentrated at the center of collector tube. In addition, the particles of ferrofluid are concentrated near the bottom side of the tube in the case of presence of magnetic field. This explains why there are vortices in Fig. 7, while in Fig. 8 such thing does not exist due to the absence of magnetic field.

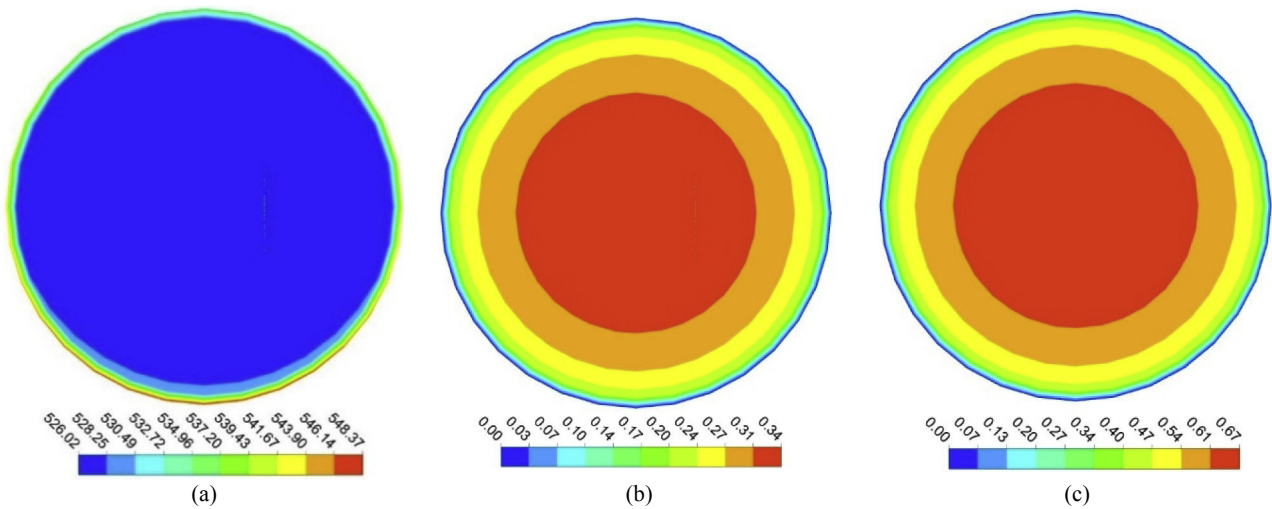


Fig. 4. (a) Outlet temperature (in K) for $Re = 15000$, (b) Velocity at $Re = 15000$ and (c) Velocity at $Re = 31000$, for base fluid (Therminol 66), $T_{in} = 503$ K.

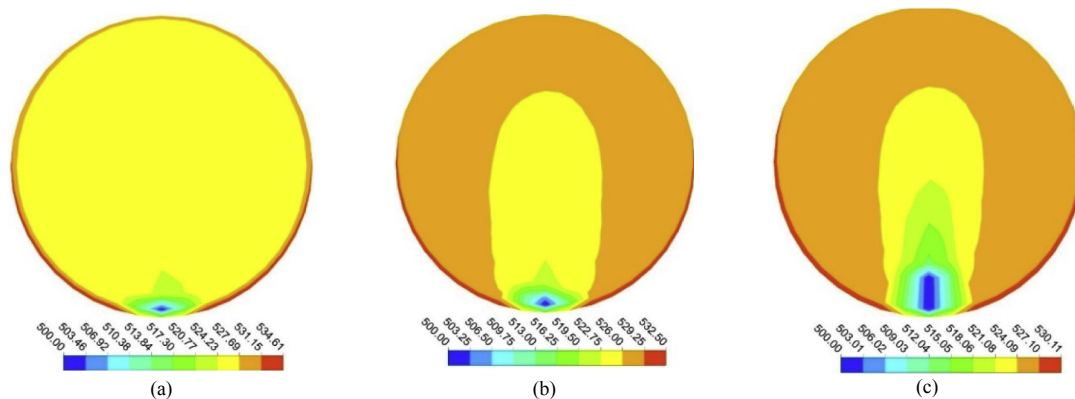


Fig. 5. Outlet temperature (in K) for $Re = 15000$, $T_{in} = 503$ K, and magnetic field of 500 G, with ferrofluid volume fraction of: (a) 1%, (b) 2%, and (c) 4%.

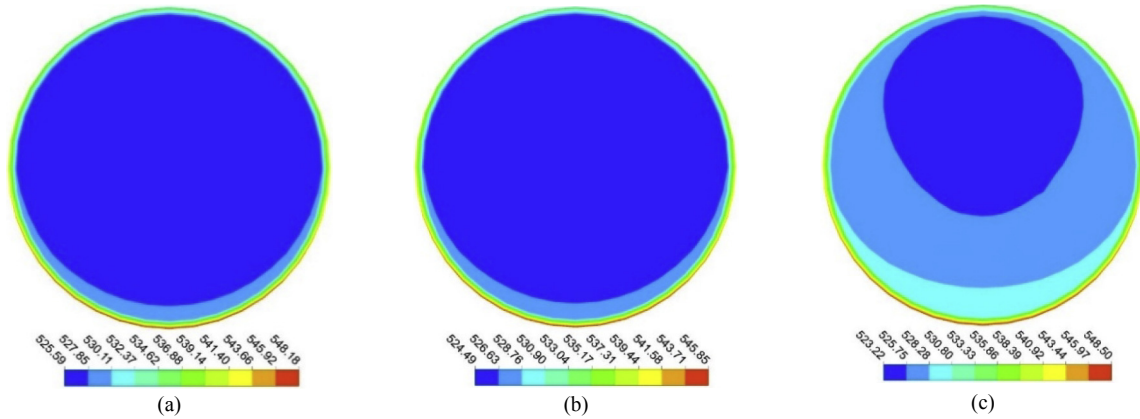


Fig. 6. Outlet temperature (in K) for $Re = 15000$, $T_{in} = 503$ K, and without magnetic field, with ferrofluid volume fraction of: (a) 1%, (b) 2%, and (c) 4%.

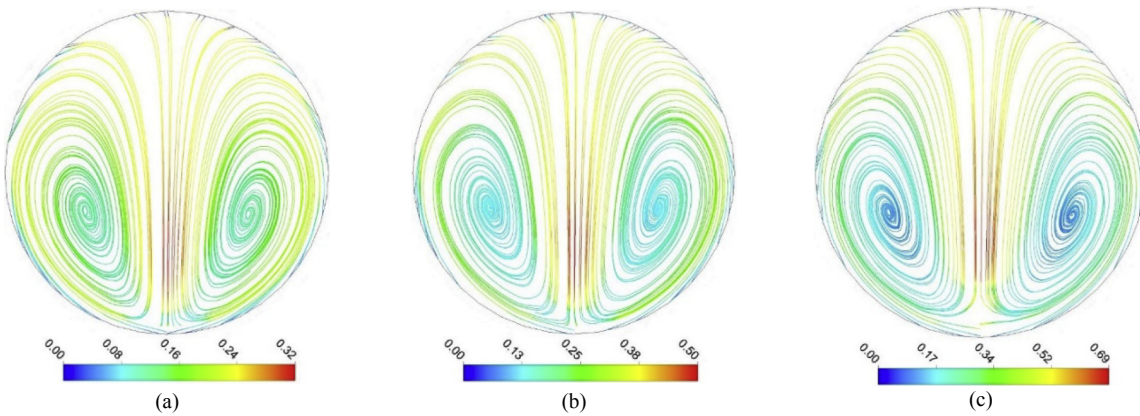


Fig. 7. Velocity profile of the ferrofluid outlet for $Re = 15000$ and magnetic field of 500 G, with ferrofluid volume fraction of: (a) 1%, (b) 2%, and (c) 4%.

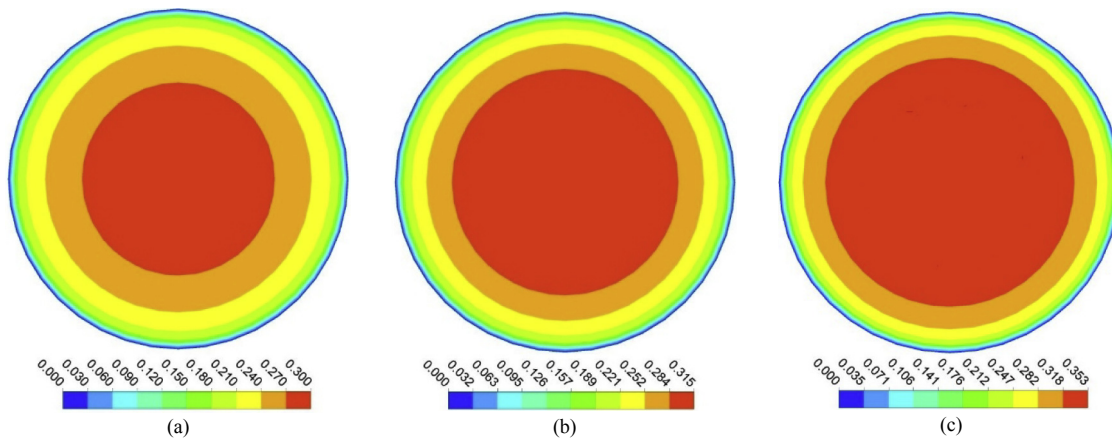


Fig. 8. Velocity profile of the ferrofluid outlet for $Re = 15000$ and without magnetic field, with ferrofluid volume fraction of: (a) 1%, (b) 2%, and (c) 4%.

Fig. 9(a) presents velocity profile of the ferrofluid with 2% volume fraction in the presence of 500G magnetic fields. The axial and cross-sectional velocities are brought in this figure in which are corresponding to outlet velocity profile were shown in Fig. 7(b). As it can be seen from this figure, the secondary flows are also forming at the middle of tube, very similar to those at the tube outlet; only their amplitude is smaller, which is according to our expectations. In addition, Fig. 9(b) and (c) show the velocity streamline and contour for ferrofluid with 2% volume fraction and $Re = 15000$, and

with magnetic field of 50 G. These figures also show that the secondary flows can have magnitudes close to the axial flow velocities, even for smaller magnetic intensities.

Fig. 10 shows the effects of transverse magnetic field on the local HTC, in which it increases with an increase in Reynolds number for ferrofluid and base fluid. First of all, as can be observed in the Fig. 10 (a), the HTC of ferrofluid (nanofluid without magnetic field) is higher than that in the base fluid. Indeed, submerged particles in the base fluid can enhance the HTC of collector tube. The HTC

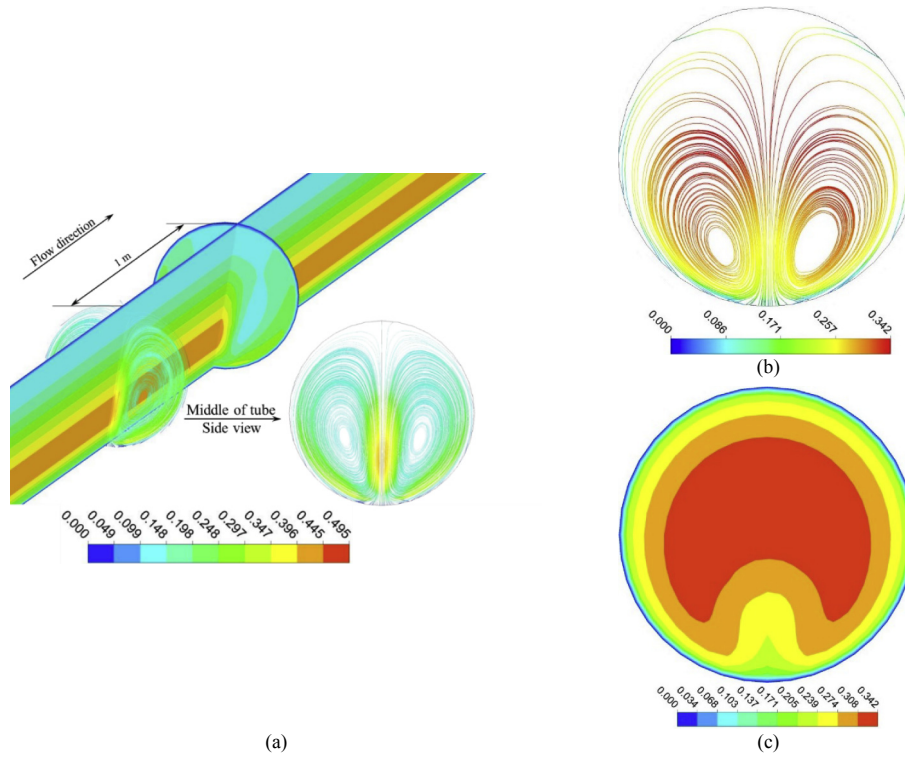


Fig. 9. Velocity profile of the ferrofluid with ferrofluid volume fraction of 2% and for $Re = 15000$, in (a) an axial and two cross-sectional planes, with magnetic field of 500 G, (b) and (c) for magnetic field of 50 G.

increases with an increase in nanoparticle volume fractions (Fig. 10(b)), which is due to have more nanoparticles in the calculation of the effective ferrofluid thermal conductivity. Application of the magnetic field increases the cooling performance of the ferrofluid. In addition, Applying non-uniform transverse magnetic field causes an increase in velocity gradient near the walls, and finally results in enhancing the heat transfer coefficient (Fig. 10(c)).

Magnetic field and nanoparticles effects on the Nusselt number variation are presented in Fig. 11. By increasing the Reynolds

number, Nusselt number experiences an increase for both ferrofluid and base fluid. Ferrofluid has the higher Nusselt number in comparison with the base fluid. Due to high thermal conductivity of nanoparticles, thermal conductivity of the ferrofluids increase, and as a result; their HTC are enhanced. By increasing the nanoparticle volume fractions, the Nusselt number increases, which is as a result of higher nanoparticle involvement in the ferrofluid effective thermal conductivity calculation.

Fig. 12 shows the variation of the friction factor for different volume fractions of ferrofluid in the collector tube, with and without presence of magnetic field. The friction factor decreases in all cases by increasing the Reynolds number. This is due to the fact

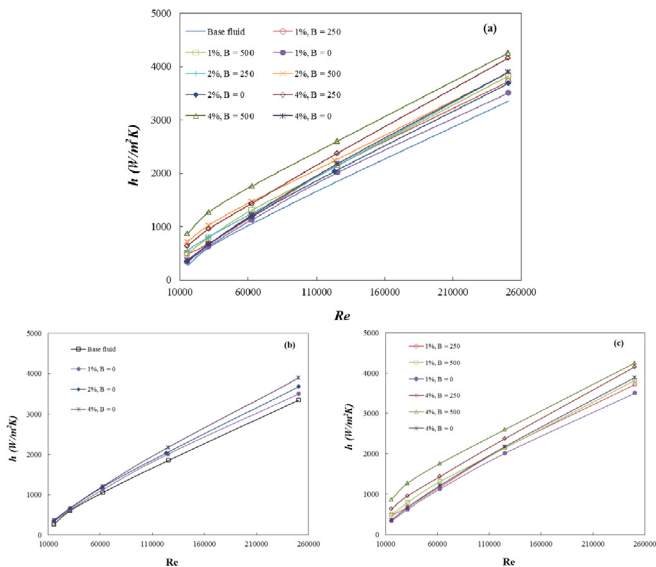


Fig. 10. Effects of magnetic field on the local convective heat transfer coefficient (h): (a) all cases, (b) without, and (c) with magnetic field only.

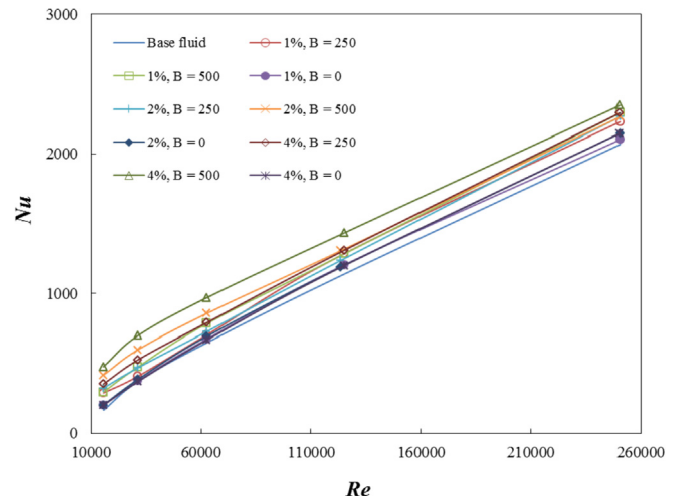


Fig. 11. Effects of magnetic field on the Nusselt number.

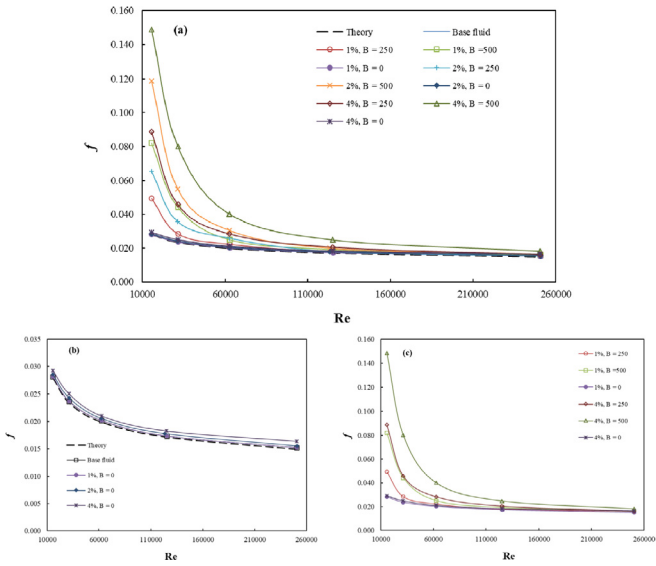


Fig. 12. Effects of magnetic field on the friction factor (f): (a) all cases, (b) without, and (c) with magnetic field only.

that the friction factor and velocity have an inverse relationship. Also, the ferrofluids have provided higher friction factor comparing to the base fluid, as a result of higher ferrofluid density and viscosity. Moreover, Fig. 12(b) shows the friction factor increase for the bigger volume fractions. In addition, magnetic field has an increasing effect on the friction factor, as can be seen in Fig. 12(c).

Variation of the pressure drop for base fluid and ferrofluid with different volume fractions, with and without presence of magnetic field is shown in Fig. 13. Dispersion of nanoparticles into the base fluid leads to an increase in ferrofluid viscosity. This leads to an increase in pressure drop of ferrofluid with bigger volume fraction. Also, increasing the Reynolds number causes a growth in pressure drop because of high velocity of the ferrofluid for the bigger Reynolds numbers. In addition, as it was shown in Fig. 7, magnetic field cause to an increase in the velocity of the ferrofluid, thus, leads to growth in the pressure drop. This is in accordance with similar conclusions presented in [44,54]. Therefore, according to Eq. (9), increase in pressure drop leads to increase in friction factor, as it was presented in Fig. 12. Although, magnetic field causes to increase in the outlet velocity as well, but rate of growth in pressure

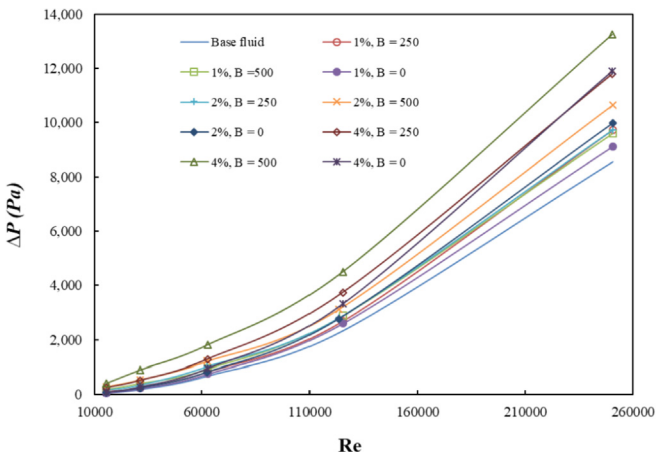


Fig. 13. Variation of pressure drop for base fluid and ferrofluid with and without magnetic field.

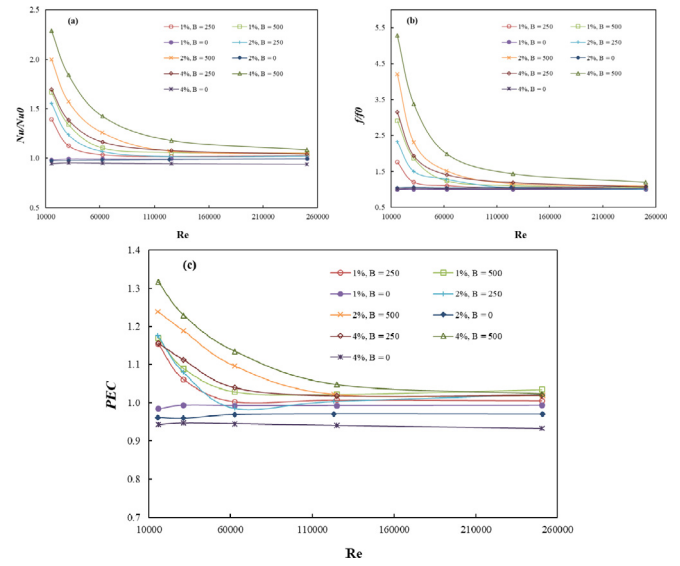


Fig. 14. Effects of magnetic field on the friction factor (f): (a) all cases, (b) without, and (c) with magnetic field only.

drop is bigger than rate of growth in velocity.

It is obvious from Eq. (11) that the value of PEC for an effective enhancement approach should be larger than unity. A larger PEC means a better thermo-hydraulic performance. Fig. 14(c) shows the variation of PEC for Fe_3O_4 -Therminol 66 ferrofluid with various volume fractions. As it can be seen from this figure, the best thermo-hydraulic performance occurs for ferrofluid with 1 vol% in the case of magnetic field absence, similar to results of Ghasemi et al. [21]. In addition, presence of magnetic field helps to have bigger HTC and friction factor, but the growth of HTCs are more than that of friction factors, which leads to have an increase in PEC for ferrofluids under magnetic field, see Fig. 14(a) and (b).

Thermal efficiency of the solar collector (η_{th}), defined by Eq. (7), is the most important parameter for its evaluation. Fig. 15 presents the variation of this parameter versus Reynolds number for the collector with base fluid and ferrofluid with various volume fractions, with and without presence of magnetic field. It can be seen from this figure that the η_{th} of collector increases for bigger volume fractions, which is due to the thermal conductivity improvement of the ferrofluids. This causes to absorb more solar radiation by the

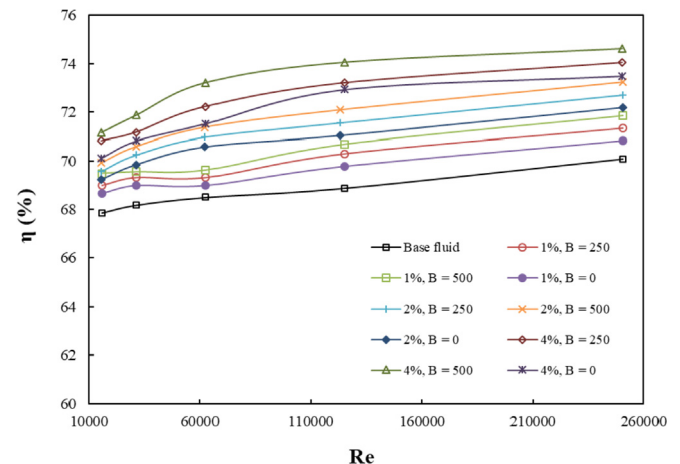


Fig. 15. Thermal efficiency of the current solar collector with different working fluids.

ferrofluid-receiver, hence more thermal energy conversion. In addition, presence of magnetic fields improves the thermal efficiency of the collector.

4. Conclusion

Current study presented a numerical study based on computational fluid dynamics incorporated within ANSYS® FLUENT®, in order to study the effects of ferrofluid and magnetic field on the performance of a parabolic trough solar collector. Fe₃O₄-Therminol 66 ferrofluid with different volume fraction was considered as the working fluid, having the Therminol 66 as the base fluid. In addition, analyses were done with and without presence of a magnetic field which was provided by a current-carrying wire located close to the collector tube. Effect of the magnetic field on the convective heat transfer coefficient, thermal efficiency, and collector performance was investigated in detail. The results have shown that the HTC of solar collector increases by using submerged nanoparticles in the base fluid. Increasing in volume fraction of nanoparticles can increase the HTC as well. Also, current investigations have shown that using magnetic field helps to increase local HTC of the collector tube, output temperature, and thermal efficiency of the collector. The best performance was obtained for ferrofluid with 4 vol% under a magnetic field of 500 G, which proves effectiveness of both ferrofluid and magnetic field on the collector performance. Finally, the best thermo-hydraulic performance occurs for ferrofluid with 1 vol% in the case of magnetic field absence for which the flow pressure drop and friction factor have the smallest values, similar to the results obtained in the literature.

Acknowledgments

The second author acknowledges support from the São Paulo State Research Foundation (FAPESP, Grant no. 2017/20994-1).

References

- [1] A. Khosravi, R.N.N. Koury, L. Machado, J.J.G. Pabon, Energy, exergy and economic analysis of a hybrid renewable energy with hydrogen storage system, *Energy* 148 (C) (2018) 1087–1102.
- [2] A. Khosravi, R.N.N. Koury, L. Machado, J.J.G. Pabon, Prediction of hourly solar radiation in Abu Musa Island using machine learning algorithms, *J. Clean. Prod.* 176 (C) (2018) 63–75.
- [3] A. Khosravi, L. Machado, R.N. Oliveira, Time-series prediction of wind speed using machine learning algorithms: a case study Osorio wind farm, Brazil, *Appl. Energy* 224 (C) (2018) 550–566.
- [4] M. Faizal, R. Saidur, S. Mekhilef, M. Alim, Energy, economic and environmental analysis of metal oxides nanofluid for flat-plate solar collector, *Energy Convers. Manag.* 76 (2013) 162–168.
- [5] U.S. Energy Information Administration Office of Integrated Analysis and Forecasting, *International Energy Outlook*, 2016.
- [6] A. Fernandez-Garcia, E. Zarza, L. Valenzuela, P.M. Erez, Parabolic-trough solar collectors and their application, *Renew. Sustain. Energy Rev.* 14 (7) (2010) 1695–1721.
- [7] E. Kaloudis, E. Papanicolaou, V. Belessiotis, Numerical simulations of a parabolic trough solar collector with nanofluid using a two-phase model, *Renew. Energy* 97 (2016) 218–229.
- [8] S. Kalogirou, The potential of solar industrial process heat applications, *Appl. Energy* 76 (4) (2003) 337–361.
- [9] V.V. Wadekar, Ionic liquids as heat transfer fluids – an assessment using industrial exchanger geometries, *Appl. Therm. Eng.* 111 (2017) 1581–1587.
- [10] E. Bellos, C. Tzivanidis, I. Daniil, K.A. Antonopoulos, The impact of internal longitudinal fins in parabolic trough collectors operating with gases, *Energy Convers. Manag.* 135 (2017) 35–54.
- [11] A. Malvandi, S. Heysiattalab, D.D. Ganji, Effects of magnetic field strength and direction on anisotropic thermal conductivity of ferrofluids (magnetic nanofluids) at filmwise condensation over a vertical cylinder, *Adv. Powder Technol.* 27 (2016) 1539–1546.
- [12] S. Choi, Enhancing thermal conductivity of fluids with nanoparticles, *ASME FED 231* (1995) 99–103.
- [13] P.J. Fule, B.A. Bhanvase, S.H. Sonawane, Experimental investigation of heat transfer enhancement in helical coil heat exchangers using water based CuO nanofluid, *Adv. Powder Technol.* 28 (9) (2017) 2288–2294.
- [14] T.P. Otanicar, P.E. Phelan, R.S. Prasher, G. Rosengarten, R.A. Taylor, Nanofluid-based direct absorption solar collector Nanofluid-based direct absorption solar collector, *Renew. Sustain. Energy* 033102 (2010), p. 033102.
- [15] A. Kasaean, S. Daviran, R.D. Azarian, A. Rashidi, Performance evaluation and nanofluid using capability study of a solar parabolic trough collector, *Energy Convers. Manag.* 89 (2015) 368–375.
- [16] T. Sokhansefat, A.B. Kasaean, F. Kowsary, Heat transfer enhancement in parabolic trough collector tube using Al₂O₃/synthetic oil nanofluid, *Renew. Sustain. Energy Rev.* 33 (2014) 636–644.
- [17] G. Xu, W. Chen, S. Deng, X. Zhang, S. Zhao, Performance evaluation of a nanofluid-based direct absorption solar collector with parabolic trough concentrator, *Nanomaterials* 5 (4) (2015) 2131–2147.
- [18] E. Bellos, C. Tzivanidis, K.A. Antonopoulos, G. Gkinis, Thermal enhancement of solar parabolic trough collectors by using nanofluids and converging-diverging absorber tube, *Renew. Energy* 94 (2016) 213–222.
- [19] B. Amina, A. Miloud, L. Samir, B. Abdelylah, J.P. Solano, Heat transfer enhancement in a parabolic trough solar receiver using longitudinal fins and nanofluids, *J. Therm. Sci.* 25 (5) (2016) 410–417.
- [20] S.E. Ghasemi, A.A. Ranjbar, Thermal performance analysis of solar parabolic trough collector using nanofluid as working fluid: a CFD modelling study, *J. Mol. Liq.* 222 (2016) 159–166.
- [21] S.E. Ghasemi, A.A. Ranjbar, Effect of using nanofluids on efficiency of parabolic trough collectors in solar thermal electric power plants, *Int. J. Hydrogen Energy* 42 (34) (2017) 21626–21634.
- [22] A. Kasaean, A.T. Eshghi, M. Sameti, A review on the applications of nanofluids in solar energy systems, *Renew. Sustain. Energy Rev.* 43 (2015) 584–598.
- [23] T.B. Gorji, A. Ranjbar, A review on optical properties and application of nanofluids in direct absorption solar collectors (DASCs), *Renew. Sustain. Energy Rev.* 72 (2017) 10–32.
- [24] N. Sandeep, Effect of aligned magnetic field on liquid thin film flow of magnetic-nanofluids embedded with graphene nanoparticles, *Adv. Powder Technol.* 28 (3) (2017) 2288–2294.
- [25] M. Alsaady, Y. Yan, and R. Boukhanouf, “An Experimental Investigation on the Effect of Ferrofluids on the Efficiency of Novel Parabolic trough Solar Collector under Laminar Flow Conditions”.
- [26] N. Gan Jia Gui, C. Stanley, N.-T. Nguyen, G. Rosengarten, Ferrofluids for heat transfer enhancement under an external magnetic field, *Int. J. Heat Mass Tran.* 123 (Aug. 2018) 110–121.
- [27] A. Jafari, T. Tynjälä, S.M. Mousavi, P. Sarkomaa, Simulation of heat transfer in a ferrofluid using computational fluid dynamics technique, *Int. J. Heat Fluid Flow* 29 (4) (2008) 1197–1202.
- [28] G. Huminic, A. Huminic, Heat transfer characteristics in double tube helical heat exchangers using nanofluids, *Int. J. Heat Mass Tran.* 54 (9) (2011) 4280–4287.
- [29] S.M. Aminossadati, A. Raisib, B. Ghasemi, Effects of magnetic field on nanofluid forced convection in a partially heated microchannel, *Int. J. Non Lin. Mech.* 46 (10) (2011) 1373–1382.
- [30] A. Malekzadeh, A. Heydarinasab, M. Jahangiri, Magnetic field effect on laminar heat transfer in a pipe for thermal entry region, *J. Mech. Sci. Technol.* 25 (4) (2011) 877–884.
- [31] H. Aminfar, M. Mohammadpourfard, Y.N. Kahnamouei, A 3D numerical simulation of mixed convection of a magnetic nanofluid in the presence of non-uniform magnetic field in a vertical tube using two phase mixture model, *J. Magn. Magn. Mater.* 323 (15) (2011) 1963–1972.
- [32] H. Aminfar, M. Mohammadpourfard, F. Mohseni, Two-phase mixture model simulation of the hydro-thermal behavior of an electrical conductive ferrofluid in the presence of magnetic fields, *J. Magn. Magn. Mater.* 324 (5) (2012) 542–830.
- [33] H. Aminfar, M. Mohammadpourfard, S.A. Zonouzi, Numerical study of the ferrofluid flow and heat transfer through a rectangular duct in the presence of a non-uniform transverse magnetic field, *J. Magn. Magn. Mater.* 327 (2013) 31–42.
- [34] H. Aminfar, M. Mohammadpourfard, Y.N. Kahnamouei, Numerical study of magnetic field effects on the mixed convection of a magnetic nanofluid in a curved tube, *Int. J. Mech. Sci.* 78 (2014) 81–90.
- [35] M. Sheikholeslami, M. Gorji-Bandpay, D.D. Ganji, Magnetic field effects on natural convection around a horizontal circular cylinder inside a square enclosure filled with nanofluid, *Int. Commun. Heat Mass Tran.* 39 (7) (2012) 978–986.
- [36] A.H. Mahmoudi, E. Abu-Nada, Combined effect of magnetic field and nanofluid variable properties on heat transfer enhancement in natural convection, *Numer. Heat Tran.* 63 (6) (2013) 452–472.
- [37] D. Yadav, J. Lee, The onset of MHD nanofluid convection with Hall current effect, *Eur. Phys. J. Plus* 130 (2015) 162.
- [38] D. Yadav, C. Kim, J. Lee, H.H. Cho, Influence of magnetic field on the onset of nanofluid convection induced by purely internal heating, *Comput. Fluids* 121 (2015) 26–36.
- [39] D. Yadav, J. Wang, R. Bhargava, J. Lee, H.H. Cho, Numerical investigation of the effect of magnetic field on the onset of nanofluid convection, *Appl. Therm. Eng.* 103 (25) (2016) 1441–1449.
- [40] A. Shakiba, K. Vahedi, Numerical analysis of magnetic field effects on hydro-thermal behavior of a magnetic nanofluid in a double pipe heat exchanger, *J. Magn. Magn. Mater.* 402 (2016) 131–142.
- [41] M. Malekan, A. Khosravi, Investigation of convective heat transfer of ferrofluid using CFD simulation and adaptive neuro-fuzzy inference system optimized

- with particle swarm optimization algorithm, *Powder Technol.* 333 (2018) 364–376.
- [42] A. Khosravi, M. Malekan, Effect of magnetic field on heat transfer coefficient of Fe₃O₄-water ferrofluid using artificial intelligence and CFD simulation, *Eur. Phys. J. Plus* (2018) 1–21.
- [43] M. Amani, P. Amani, A. Kasaeian, O. Mahian, S. Wongwises, Thermal conductivity measurement of spinel-type ferrite MnFe₂O₄ nanofluids in the presence of a uniform magnetic field, *J. Mol. Liq.* 230 (2017) 121–128.
- [44] M. Amani, M. Ameri, A. Kasaeian, The experimental study of convection heat transfer characteristics and pressure drop of magnetite nanofluid in a porous metal foam tube, *Transport Porous Media* 116 (2) (2017) 959–974.
- [45] R. Hamilton, O. Crosser, Thermal conductivity of heterogeneous two-component systems, *Ind. Eng. Chem. Fundam.* 1 (3) (1962) 187–191.
- [46] E. Shojaeizadeh, F. Veysi, A. Kamandi, Exergy efficiency investigation and optimization of an Al₂O₃-water nanofluid based flat-plate solar collector, *Energy Build.* 101 (2015) 12–23.
- [47] A. Khosravi, R. N. N. Koury, and L. Machado, "Thermo-economic analysis and sizing of the components of an ejector expansion refrigeration system," *Int. J. Refrig.*, vol. 86, pp. 463–479, Feb.
- [48] E. Bellos, C. Tzivanidis, D. Tsimpoukis, Thermal enhancement of parabolic trough collector with internally finned absorbers, *Sol. Energy* 157 (July) (2017) 514–531.
- [49] B.S. Petukhov, Heat transfer in turbulent pipe flow with variable physical properties, in: J.P. Harnett (Ed.), *Adv. Heat Transf.*, vol. 6, 1970, pp. 504–564.
- [50] R. Webb, Performance evaluation criteria for use of enhanced heat transfer surfaces in heat exchanger design, *Int. J. Heat Mass Tran.* 24 (1981) 715–726.
- [51] E. Tzirtzilakis, N. Kafoussias, Three-dimensional magnetic fluid boundary layer flow over a linearly stretching sheet, *J. Heat Tran.* 132 (1) (2010), 011702.
- [52] E.D. Koronaki, H.H. Liakos, M.A. Founti, N.C. Markatos, Numerical study of turbulent diesel flow in a pipe with sudden expansion, *Appl. Math. Model.* 25 (2001) 319–333.
- [53] B. Zheng, C.X. Lin, M.A. Ebadian, Combined turbulent forced convection and thermal radiation in a curved pipe with uniform wall temperature, *Numer. Heat Transf. A Appl.* 44 (2003) 149–167.
- [54] S. Ahangar Zonouzi, et al., Experimental investigation of the flow and heat transfer of magnetic nanofluid in a vertical tube in the presence of magnetic quadrupole field, *Exp. Therm. Fluid Sci.* 91 (2018).